Ideal Metals

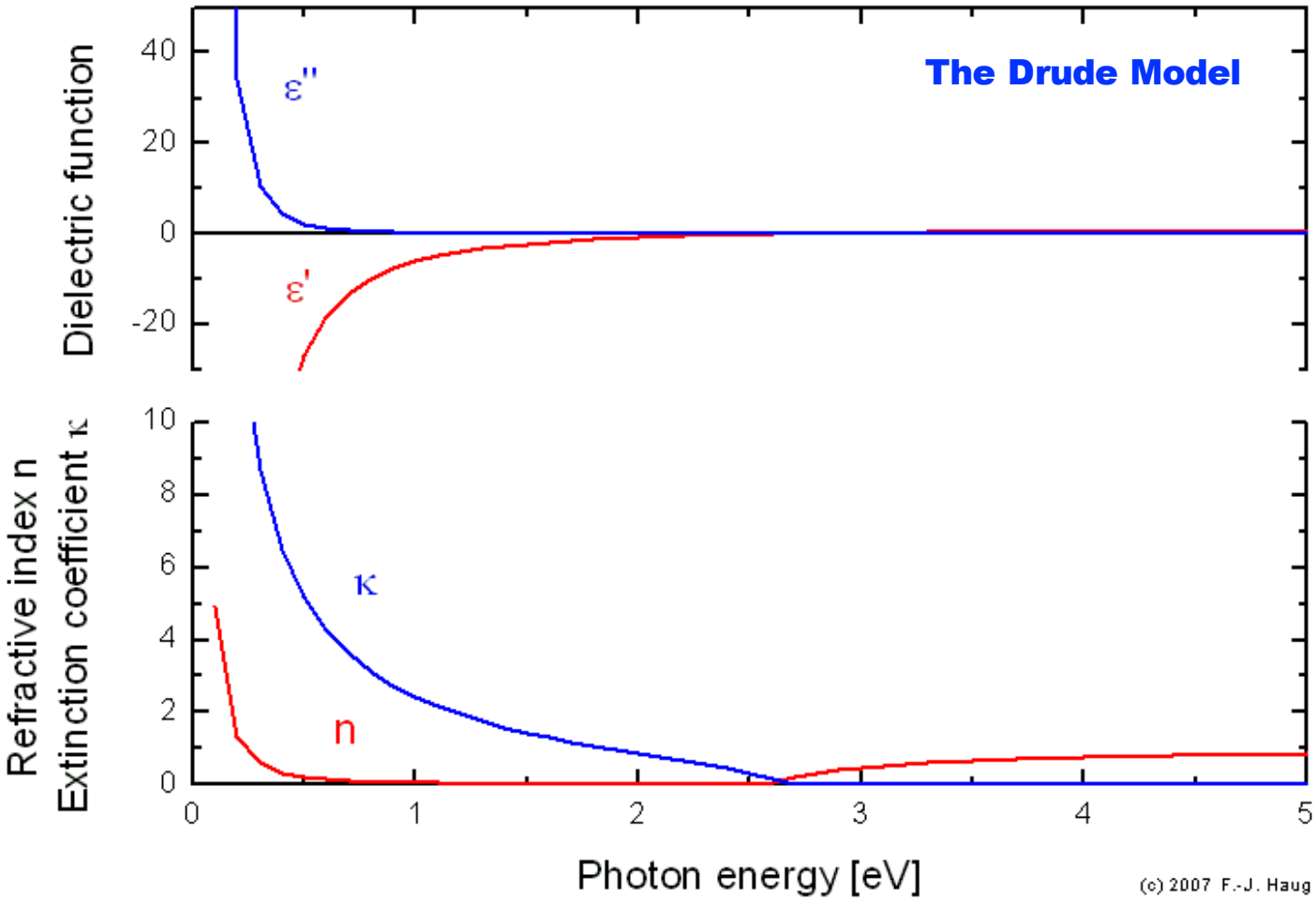

From the diagram we observe that ϰ should become small for frequencies higher than the plasma frequency, i.e. the electron gas behaves like a dielectic and becomes transparent. In reality this is not completely true, the figure below shows the dielectric functions for two real metals, silver (black) and gold (red).

Real Metals

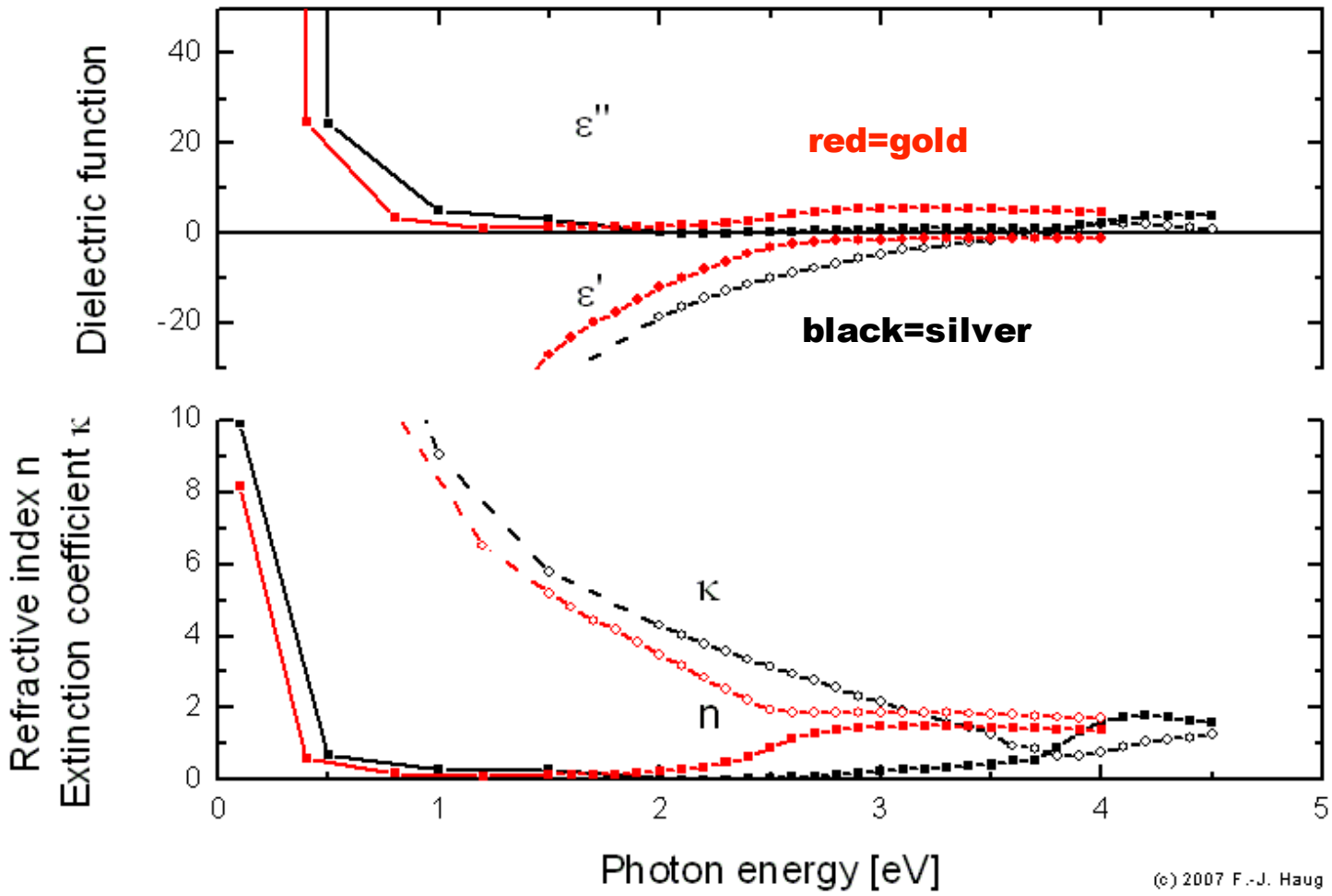
Dielectric function
40
20
0
-20
ε''
ε'
red=gold
black=silver
Refractive index n
Extinction coefficient κ
10
8
6
4
2
0
κ
n
0
1
2
3
4
5
Photon energy [eV]
(c) 2007 F.-J. Haug

Ideal Dielectrics

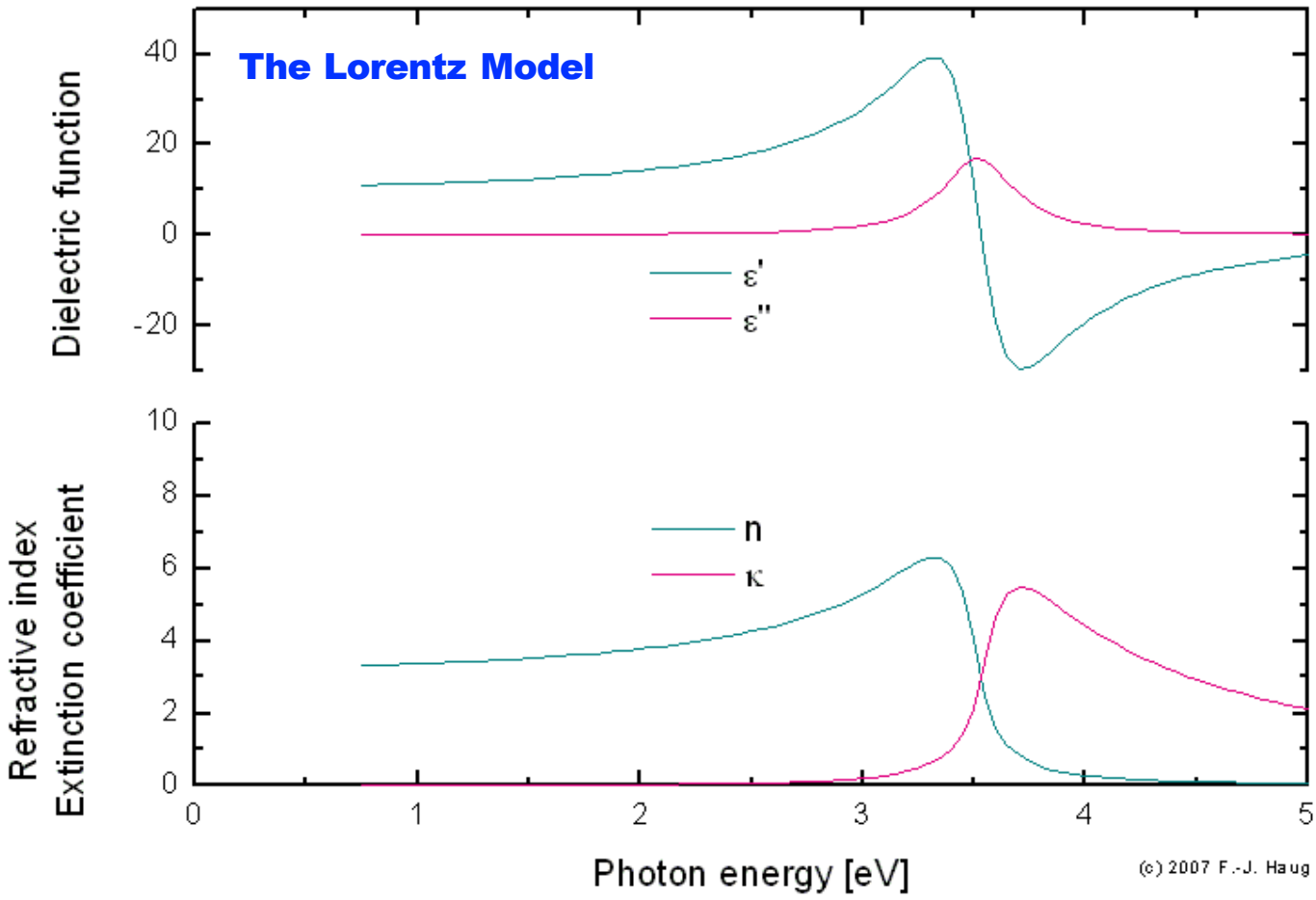

Real Dielectric (silicon)

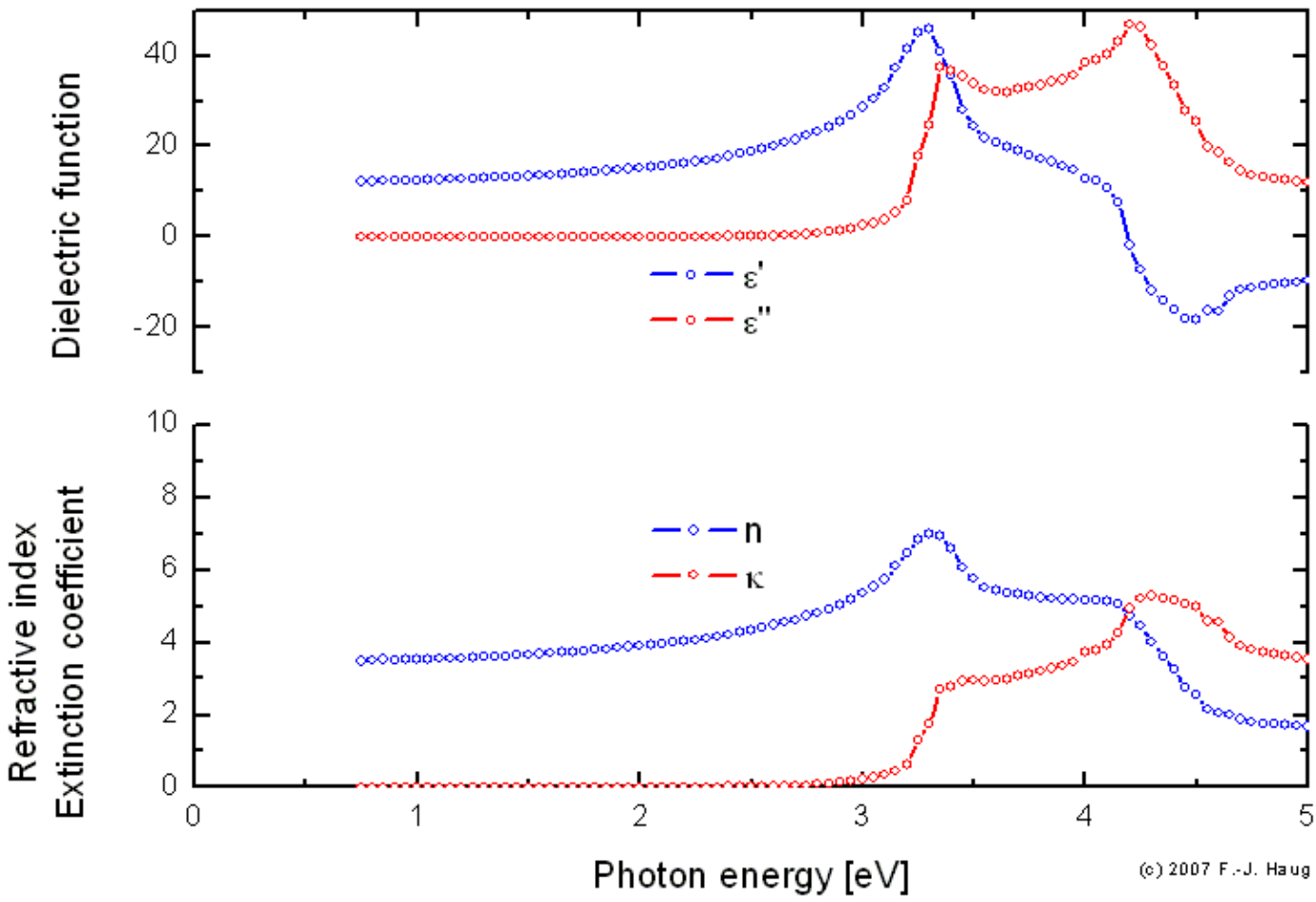

Chapter 3

ABSORPTION AND DISPERSION

This chapter consists mostly of a rather elementary treatment of absorption and dispersion. It includes some simple examples of applications to optical properties and photoemission.

The classical theory of absorption and dispersion is due mainly to Lorentz and Drude. The Lorentz model is applicable to insulators; its quantum mechanical analog includes all direct interband transitions; i.e., all transitions for which the final state of an electron lies in a different band but with no change in **k**-vector in the reduced zone scheme. The Drude model is applicable to free-electron metals; its quantum mechanical analog includes intraband transitions, where intraband transitions are taken to mean all transitions not involving a reciprocal lattice vector.

Both the Lorentz and Drude models are largely *ad hoc*, but still useful as starting points and for developing a feeling for optical properties. We shall see that many features of these classical models have quantum mechanical counterparts which are easily understood as generalizations of their classical analogs.

3.1 The Lorentz Oscillator

Consider an atom with electrons bound to the nucleus in much the same way as a small mass can be bound to a large mass by a spring. This is the Lorentz model. The motion of an electron bound to the nucleus is then

described by

$$m\frac{d^2\mathbf{r}}{dt^2} + m\Gamma\frac{d\mathbf{r}}{dt} + m\omega_0{}^2\mathbf{r} = -e\mathbf{E}_{\text{loc}} \tag{3.1}$$

where m is the electronic mass and e is the magnitude of electronic charge. The field $\mathbf{E}_{\text{loc}}$ is the local electric field acting on the electron as a driving force. It is a microscopic field but is written as $\mathbf{E}_{\text{loc}}$ to eliminate confusion with the electronic charge $-e$ and to conform with common usage. The term $m\Gamma(d\mathbf{r}/dt)$ represents viscous damping and provides for an energy loss mechanism. The actual loss mechanism is radiation damping for a free atom, but it arises from various scattering mechanisms in a solid. The damping term in Eq. (3.1) is written in the form in which it often appears in describing the electrical conductivity metals. The term $m\omega_0{}^2\mathbf{r}$ is a Hooke's law restoring force.

In the context of a classical model, there are two approximations in Eq. (3.1). The nucleus has been assumed to have infinite mass, otherwise the reduced mass should have been used. We could have simply included the reduced mass, but our goal is to understand solids and there we can quite accurately take the mass of the lattice as infinite. We have also neglected the small force $-e\mathbf{v} \times \mathbf{b}/c$ arising from the interaction of the electron with the magnetic field of the light wave. It is negligible because the velocity of the electron is small compared with c.

The local field can be taken to vary in time as $e^{-i\omega t}$; thus the solution to Eq. (3.1) is

$$\hat{\mathbf{r}} = \frac{-e\mathbf{E}_{\text{loc}}/m}{(\omega_0{}^2 - \omega^2) - i\Gamma\omega} \tag{3.2}$$

and the induced dipole moment is

$$\hat{\mathbf{p}} = \frac{e^2\mathbf{E}_{\text{loc}}}{m}\frac{1}{(\omega_0{}^2 - \omega^2) - i\Gamma\omega} \tag{3.3}$$

Note that it is important to be consistent in the form of the time variation used to describe time-dependent fields. The use of a time variation $e^{i\omega t}$ leads to a complex refractive index $\hat{n} = n - ik$ rather than the convention $\hat{n} = n + ik$ chosen earlier.

We now assume that the displacement r is sufficiently small that a linear relationship exist between $\hat{\mathbf{p}}$ and $\mathbf{E}_{\text{loc}}$, namely

$$\hat{\mathbf{p}} = \hat{\alpha}(\omega)\mathbf{E}_{\text{loc}} \tag{3.4}$$

where $\hat{\alpha}(\omega)$ is the frequency-dependent atomic polarizability. From Eqs.

(3.3) and (3.4), the polarizability for a one-electron atom is seen to be

$$\hat{\alpha}(\omega) = \frac{e^2}{m} \frac{1}{(\omega_0{}^2 - \omega^2) - i\Gamma\omega} \tag{3.5}$$

The polarizability is complex because of the inclusion of a damping term. As a result, the polarization differs in phase from the local field at all frequencies.

If there are N atoms per unit volume, the macroscopic polarization is

$$\mathbf{P} = N\langle \mathbf{p} \rangle = N\hat{\alpha}\langle \mathbf{E}_{\text{loc}} \rangle = \chi_e \mathbf{E} \tag{3.6}$$

To relate the microscopic atomic polarizability to the macroscopic electric susceptibility, it is necessary to know the relationship between the microscopic field $\mathbf{E}_{\text{loc}}$ and the macroscopic field $\mathbf{E}$. Except for some limiting ideal cases, this is a problem of considerable complexity. It is discussed briefly in Appendix B. In general, $\langle \mathbf{E}_{\text{loc}} \rangle \neq \mathbf{E}$ since $\langle \mathbf{E}_{\text{loc}} \rangle$ is usually an average over atomic sites, not over regions between sites. For free-electron metals, though, we can argue that since the conduction electrons are not bound, the field felt by the conduction electrons is on the average just the macroscopic field $\mathbf{E}$. Then, of course, we should let $\omega_0 = 0$ in Eq. (3.1) because the conduction electrons are not bound. The result is just the Drude model for metals. However, what we shall do is something in between. We will keep the restoring force term, but still assume for simplicity that $\langle \mathbf{E}_{\text{loc}} \rangle = \mathbf{E}$. Such a model contains all the essential features to describe the optical properties; but it must be remembered that in the detailed analysis of specific real solids, it is necessary to consider carefully what is the correct field to use. Proceeding with our assumptions, then, we have

$$\hat{\mathbf{P}} = N\hat{\alpha}\mathbf{E} = \chi_e \mathbf{E} \tag{3.7}$$

We are now ready to get an expression for the dielectric function in terms of the atomic polarizability. But we now have an energy loss mechanism explicitly included with the result that the atomic polarizability is now complex. This means also that the fields $\mathbf{E}$, $\mathbf{P}$, and $\mathbf{D}$ are not in phase. The most convenient way to handle the situation is to generalize some earlier results. In analogy with Eq. (2.67), we define a complex displacement $\hat{\mathbf{D}}$ such that

$$\hat{\mathbf{D}} = \hat{\varepsilon}\mathbf{E} = \mathbf{E} + 4\pi\hat{\mathbf{P}} = \hat{\mathbf{E}}^{\text{ext}} \tag{3.8}$$

This is equivalent to defining $\hat{\mathbf{D}}$ as

$$\hat{\mathbf{D}} = \mathbf{D} + i(4\pi/\omega)\,\mathbf{J} \tag{3.9}$$

The physical quantities $\mathbf{E}$, $\mathbf{D}$, $\mathbf{J}$, etc. are generally written in complex nota-

tion as, e.g.,

$$\mathbf{D} = \mathbf{D}_0 \exp i(\mathbf{q} \cdot \mathbf{r} - \omega t) \tag{3.10}$$

because this notation explicitly shows the phase, in addition to greatly simplifying the mathematical manipulations. Values for these physical quantities are obtained by taking the real part of the complex expressions used for these quantities. Although $\hat{\mathbf{D}}$ can also be written in complex notation, the values for the physical quantities that $\hat{\mathbf{D}}$ represents are not obtained by taking the real part of $\hat{\mathbf{D}}$. The quantity $\hat{\mathbf{D}}$ is truly a complex quantity and represents the two real quantities $\mathbf{D}$ and $\mathbf{J}$. The true values for $\hat{\mathbf{D}}$ must be obtained from the right-hand side of Eq. (3.9) by taking the real parts of $\mathbf{D}$ and $\mathbf{J}$, i.e.,

$$\hat{\mathbf{D}}(\text{true}) = \text{Re}(\hat{\mathbf{D}}) + i(4\pi/\omega)\,\text{Re}(\mathbf{J}) \tag{3.11}$$

Having recognized that there is a truly complex $\hat{\mathbf{D}}$, we shall from here on generally follow convention and write simply $\mathbf{D}$. We shall explicitly designate complex quantities only for properties of the medium, e.g., the complex dielectric function $\hat{\varepsilon}$ and the complex polarizability $\hat{\alpha}$.

Now, from Eqs. (3.7) and (3.8), we get

$$\hat{\varepsilon} = 1 + 4\pi N\hat{\alpha} \tag{3.12}$$

Using Eq. (3.5), this becomes

$$\hat{\varepsilon} = 1 + \frac{4\pi Ne^2}{m} \frac{1}{(\omega_0{}^2 - \omega^2) - i\Gamma\omega} \tag{3.13}$$

From Eq. (3.13) and the definitions is Eqs. (2.89)–(2.91), we get, for non-magnetic materials,

$$\varepsilon_1 = n^2 - k^2 = 1 + \frac{4\pi Ne^2}{m} \frac{(\omega_0{}^2 - \omega^2)}{(\omega_0{}^2 - \omega^2)^2 + \Gamma^2\omega^2} \tag{3.14}$$

$$\varepsilon_2 = 2nk = \frac{4\pi Ne^2}{m} \frac{\Gamma\omega}{(\omega_0{}^2 - \omega^2)^2 + \Gamma^2\omega^2} \tag{3.15}$$

If we consider classical atoms with more than one electron per atom, we can extend the previous results. Let N_j be the density of electrons bound with resonance frequency ω_j. Then,

$$\hat{\varepsilon} = 1 + \frac{4\pi e^2}{m} \sum_j \frac{N_j}{(\omega_j{}^2 - \omega^2) - i\Gamma_j\omega} \tag{3.16}$$

$$\sum_j N_j = N \tag{3.17}$$

We shall shortly derive a corresponding quantum mechanical equation which can be written

$$\hat{\varepsilon} = 1 + \frac{4\pi e^2}{m} \sum_j \frac{Nf_j}{(\omega_j^2 - \omega^2) - i\Gamma_j\omega} \tag{3.18}$$

There is a formal similarity between Eqs. (3.16) and (3.18), but the meanings of some corresponding terms are quite different. In Eq. (3.16), ω_j is the resonance frequency of a bound electron, whereas in Eq. (3.18), it is the transition frequency of an electron between two atomic states separated in energy by $\hbar\omega_j$. The parameter f_j, called the oscillator strength, is a measure of the relative probability of a quantum mechanical transition. We shall show that for free atoms, it satisfies a sum rule

$$\sum_j f_j = 1 \tag{3.19}$$

which is the quantum mechanical analogy to Eq. (3.17).

Now, return to Eqs. (3.14) and (3.15) and consider the frequency dependence of ε_1 and ε_2 for a solid made of a collection of single-electron classical atoms. The frequency dependence is illustrated graphically in Fig. 3.1.

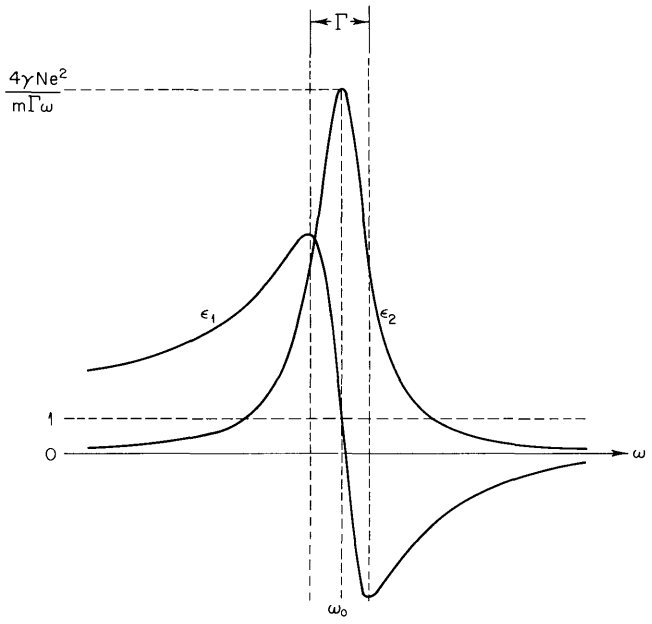

Fig. 3.1 Frequency dependence of ε_1 and ε_2.

Figure 3.1 shows that except for a narrow region near ω_0, ε_1 increases with increasing frequency. This is called normal dispersion. However, there is a region near ω_0 where ε_1 decreases with increasing frequency. This is called anomalous dispersion. We can find the width of the region of anomalous dispersion as follows. Equating the derivative of Eq. (3.14) to zero, we find

$$(\omega_0^2 - \omega_m^2)^2 = \pm \omega_0^2 \Gamma^2 \tag{3.20}$$

where ω_m is the frequency at which ε_1 is a maximum or a minimum. If the region of anomalous dispersion is reasonably narrow, $\omega_m \approx \omega_0$,

$$(\omega_0 - \omega_m) = \pm \Gamma/2 \tag{3.21}$$

and the full width of the region of anomalous dispersion is Γ. In the absence of an energy loss mechanism, there is a singularity at ω_0.

If

$$\Gamma \approx 0 \tag{3.22}$$

ε_2 versus ω is a bell-shaped curve which is symmetric about ω_0. Small values of Γ compared with ω_0 cause little distortion. From Eq. (3.15), we find that the maximum value of ε_2 is

$$\varepsilon_2(\text{max}) = \frac{4\pi Ne^2/m}{\Gamma\omega_0} \tag{3.23}$$

assuming the maximum occurs exactly at ω_0. Also, the full width of the ε_2 curve at half maximum is Γ.

Figure 3.1 shows the contribution of the electronic polarizability to the dielectric constant. There are also other contributions. For example, in ionic crystals, in the infrared region, there is an absorption spectrum and polarization associated with the direct stimulation of vibrational modes of the ions by means of electromagnetic radiation. The Lorentz model also describes that situation.

Figure 3.2 shows the general form of the polarizability to be expected

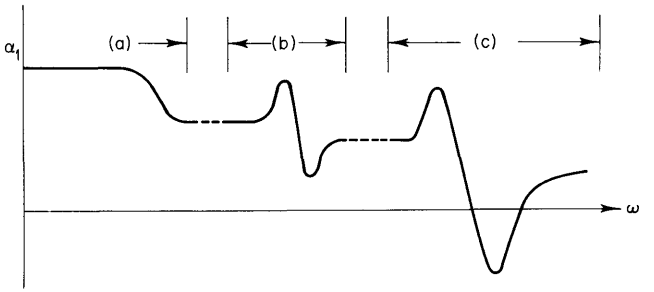

Fig. 3.2 Frequency dependence of contributions to the polarizability arising from orientation of (a) permanent dipoles (microwave), (b) ionic lattice vibrations (infrared), and (c) displacement of electrons (visible and ultraviolet).

in a material consisting of three discrete modes of oscillation. Although all the modes of oscillation contribute to the polarizability and to the dielectric constant, the contributions of ionic motions are small at optical frequencies because of the large inertia of ions compared with electrons. We shall consider only electronic contributions to the dielectric constant. In that context, references to the low-frequency dielectric constant of a material will mean the dielectric constant at the low-frequency end of the visible region but at a frequency high compared with lattice vibrations or molecular oscillations in the crystal.

We now want to consider the implications of the frequency dependence of ε_1 and ε_2 for the optical properties of solids. The reflectivity of solids at normal incidence is shown in Appendix C to be given by

$$R = \frac{(n-1)^2 + k^2}{(n+1)^2 + k^2} \tag{3.24}$$

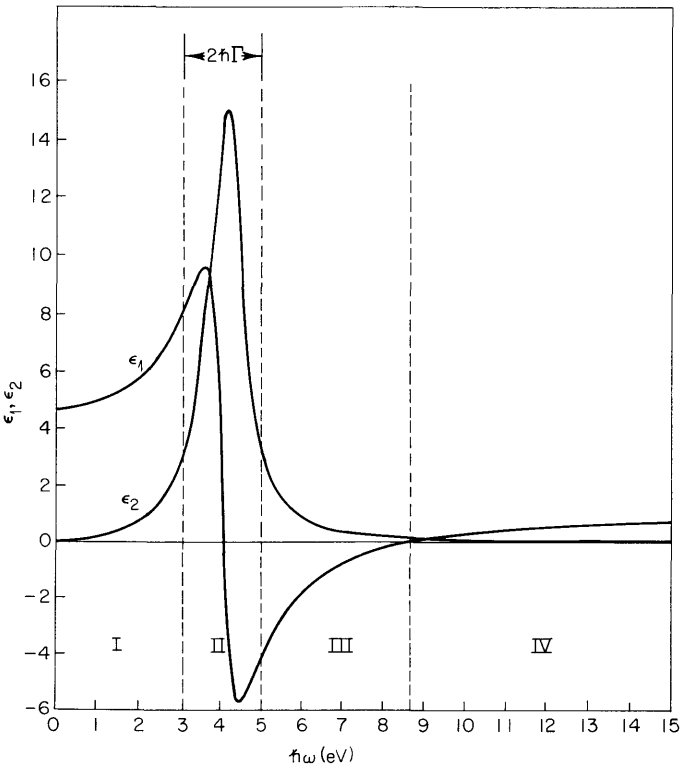

Fig. 3.3 Spectral dependence of ε_1 and ε_1. The curves are calculated for the case in which $\hbar\omega_0 = 4$ eV, $\hbar\Gamma = 1$ eV, and $4\pi Ne^2/m = 60$. The onset of region IV is defined by $\varepsilon_1 = 0$.

Using Eqs. (2.90) and (2.91), we find that for nonmagnetic materials,

$$n = \{\tfrac{1}{2}[(\varepsilon_1{}^2 + \varepsilon_2{}^2)^{1/2} + \varepsilon_1]\}^{1/2} \tag{3.25}$$

$$k = \{\tfrac{1}{2}[(\varepsilon_1{}^2 + \varepsilon_2{}^2)^{1/2} - \varepsilon_1]\}^{1/2} \tag{3.26}$$

Now, from Eqs. (3.14), (3.15), and (3.24)–(3.26), we can analyze the frequency-dependent behavior of a solid in terms of whether it is primarily reflecting, absorbing, or transparent. The results are summarized in Figs. 3.3–3.5.

In region I, $\omega \ll \omega_0$, $\varepsilon_2 = 2nk = 0$, and $\varepsilon_1 = n^2 - k^2 > 1$. We may thus conclude that $k = 0$, $n > 1$, and $\varepsilon_1 = n^2$.

Insulators, such as KCl, typically have a refractive index of about 1.5 in region I. Thus, region I is characterized by high transparency, no absorption, and a small reflectivity for insulators. This is illustrated in Fig.

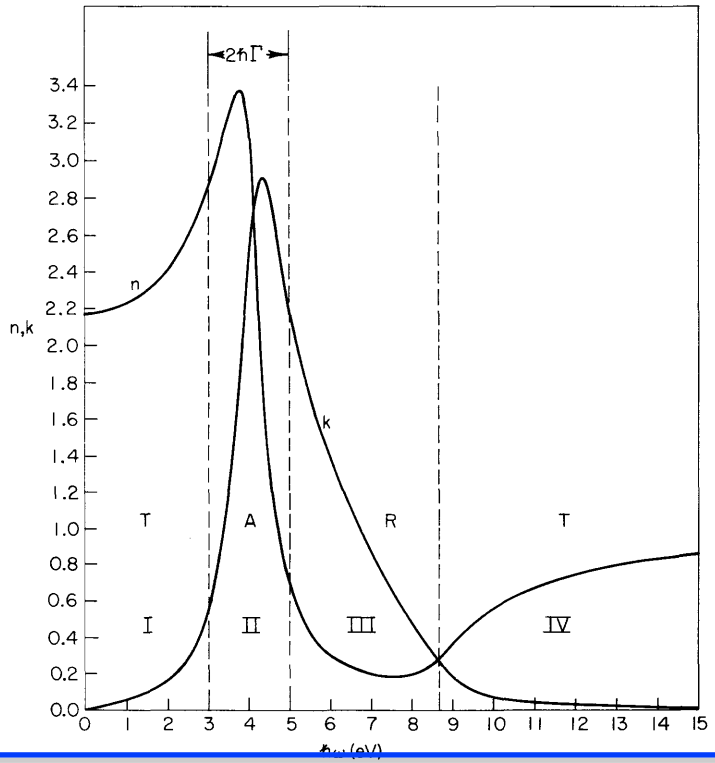

Fig. 3.4 Spectral dependence of n and k. The curves are calculated from the values of ε_1 and ε_2 given in Fig. 3.3. The regions I, II, III, and IV can be seen to be primarily transmitting (T), absorbing (A), reflecting (R), and transmitting (T), respectively. These results follow from consideration of Eq. (3.24) and the realization that strong absorption takes place only in the neighborhood of a transition frequency.

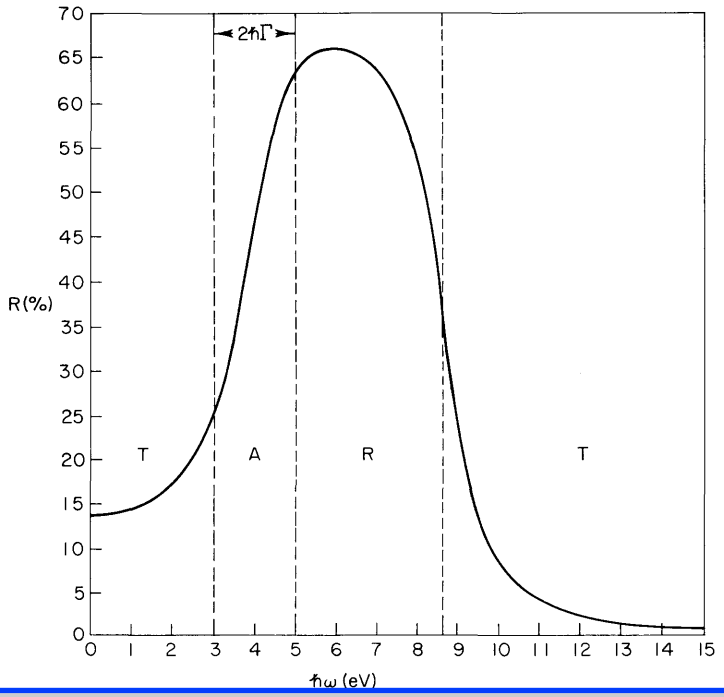

Fig. 3.5 Spectral dependence of reflectivity. The curve is calculated from the n and k values given in Fig. 3.4.

3.6 for the reflectivity of KCl. Of course, since the treatment developed here does not include local field corrections, it is not quantitatively applicable to highly ionic materials. However, for highly polarizable materials such as Si and Ge, there is probably no need to include local field corrections.

The difficulty with applying the present formulas to real materials, even in the absence of local field corrections, is that real materials correspond to a collection of Lorentz oscillators with different frequencies spread out over bands. Nonetheless, if we think of the frequency of a Lorentz oscillator as corresponding to the transition frequency across the band gap of an insulator or semiconductor, we can make some estimates of the optical properties. We can even include approximate band structure effects by using an effective mass rather than the free-electron mass. For example, Fig. 3.7 shows that the reflectivity of Si rises sharply at about 3 eV. This corresponds to a frequency $\omega_0 = 4.5 \times 10^{15}$ sec^{-1}. If we take this as an approximate value for the average spring frequency to be used in Eq. (3.14), and assume four valence electrons per Si atom, each with the mass of a free electron, then $\varepsilon_1(\omega \to 0) = 15$. That is in fairly good agreement with the experimental low-frequency value $\varepsilon_1 = 12$.

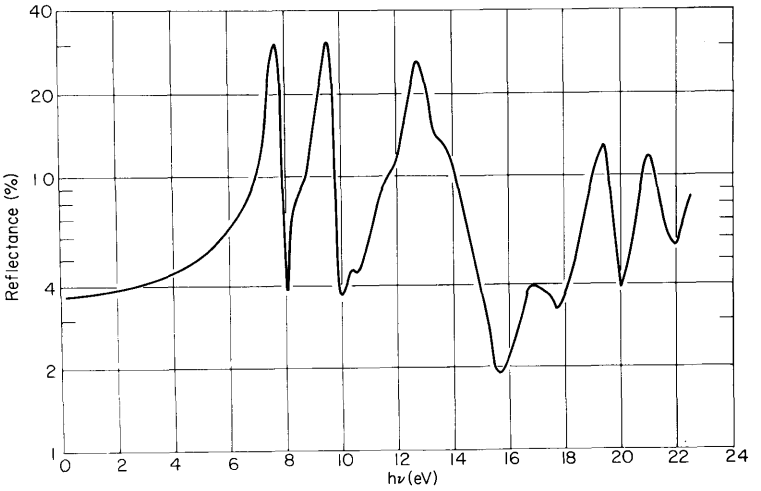

Fig. 3.6 The spectral dependence of the reflectance of KCl. The region of transparency extends to about 7 eV. Above 7 eV, there are a number of sharp peaks related to narrow energy bands and excitons. [From H. R. Philipp and H. Ehrenreich, *Phys. Rev.* **131**, 2016 (1963).]

The refractive index for more highly polarizable materials such as Si and Ge is higher than for ionic insulators. For Si, $n = 3.5$, and for Ge at low frequencies, $n = 4$. As a result, the reflectivity can be appreciable in region I even though there is no absorption. The reflectivity arises from the induced polarization current corresponding to the valence electrons oscillating out of phase with the incident radiation. There is no absorption for this process, but the interference of the incident beam with the waves reradiated by the valence electrons does lead to appreciable reflectivity.

That the Lorentz model is qualitatively correct for semiconductors and insulators is also indicated by the dependence of ε_1 on band gap. Thus, if we identify $\hbar\omega_0$ as corresponding approximately to the band gap, then ε_1 should decrease with increasing band gap. That indeed is the case. The band gaps of Ge, Si and KCl are, respectively, 0.8, 1.1, and 7.5 eV, whereas the low-frequency optical dielectric constants are, respectively, 4, 3.5, and 1.5.

Region II of Figs. 3.3–3.5 is characterized by strong absorption. There may also be appreciable reflectivity in this region. That simply means that although the values of n and k may be high, leading to appreciable reflectivity, the light that is not reflected is strongly absorbed in the material.

In region III, $\omega \gg \omega_0$, and the electrons of the insulator respond as if they were free electrons. This is because the photon energy is much greater than the binding energy of the electron. The insulator thus has a metallic reflectance. Of course, for good insulators, this region lies well into the vacuum-ultraviolet and cannot be observed visually. However, for semi-

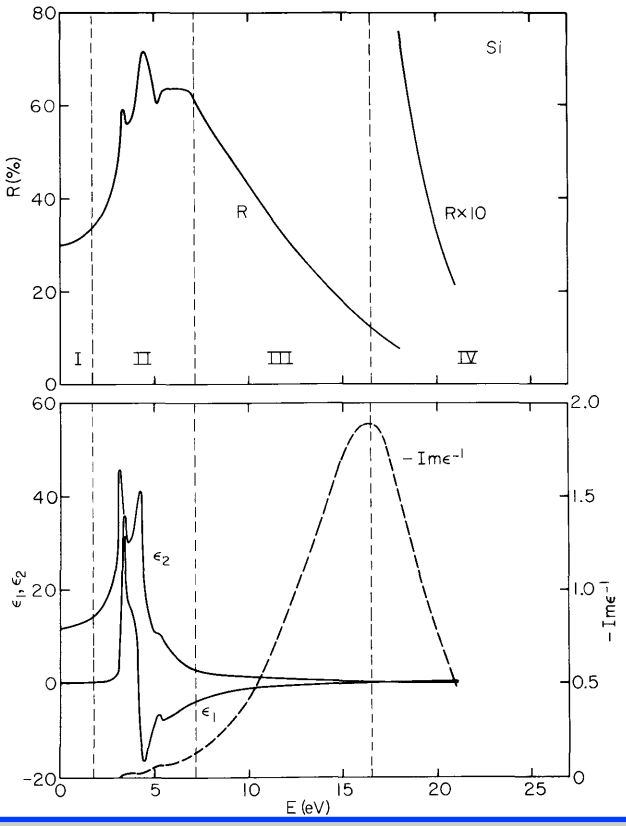

Fig. 3.7 The spectral dependence of the reflectance and dielectric functions of Si. Regions I, II, III, and IV correspond to the regions with the same designation shown in Figs. 3.1, 3.3, and 3.4. [H. R. Philipp and H. Ehrenreich, *Phys. Rev.* **129**. 1550 (1963).]

conductors like Ge and Si, the band gap lies in the infrared and the region of metallic reflectance is in the visible. Thus, KCl is transparent to the eye, but Ge and Si have a metallic appearance.

The onset of region IV is defined by $\varepsilon_1 = 0$. This happens at a frequency ω_p called the plasma frequency. From Eq. (3.14), assuming $\omega \gg \omega_0 \gg \Gamma$, we find

$$\omega_p^2 = 4\pi Ne^2/m \tag{3.27}$$

3.2 The Drude Model for Metals

The Drude model for metals is obtained directly from the Lorentz model for insulators simply by equating the restoring force to zero. The conduction

electrons of a metal are not bound. Furthermore, because the wave function for a free electron is distributed fairly uniformly throughout the metal, the field acting on the electron is just the average field. Thus, there is no need to make corrections for the local field.

From Eqs. (3.14) and (3.15), taking $\omega_0 = 0$, we have

$$\varepsilon_1 = 1 - \frac{4\pi Ne^2}{m} \frac{1}{(\omega^2 + \Gamma^2)} \tag{3.28}$$

$$\varepsilon_2 = \frac{4\pi Ne^2}{m} \frac{\Gamma}{\omega(\omega^2 + \Gamma^2)} \tag{3.29}$$

The origin of the viscous damping term for a free-electron metal is the ordinary scattering of electrons associated with electrical resistivity. In the next chapter, when we derive the properties of a free-electron metal in terms of a complex conductivity rather than a complex dielectric function, we shall see that $\Gamma = \tau^{-1}$, where τ is the mean free time between collisions. If we now make the substitution $\Gamma = \tau^{-1}$, and use Eq. (3.27), we get from Eqs. (3.28) and (3.29)

$$\varepsilon_1 = 1 - \frac{\omega^2\tau^2}{(1 + \omega^2\tau^2)} \tag{3.30}$$

$$\varepsilon_2 = \frac{\omega_p{}^2\tau}{\omega(1 + \omega^2\tau^2)} \tag{3.31}$$

Since the Drude model is obtained directly from the Lorentz model simply by setting ω_0 equal to zero, the optical properties of a free-electron metal should resemble those for an insulator at frequencies greater than ω_0. As we saw in the preceding section, the frequency range $\omega > \omega_0$ in an insulator corresponds to the region in which the electrons are effectively free, so that it might be more accurate to say that an insulator responds like a metal to photons of energy $\hbar\omega > \hbar\omega_0$.

A plot of the dielectric functions and the optical constants for a Drude metal is shown in Figs. 3.8–3.10. The corresponding reflectivity is shown in Fig. 3.11. It is clear from Fig. 3.11 that for an ideal free-electron metal, the reflectivity approaches unity below the plasma frequency. Above the plasma frequency, the metal is transparent and the reflectivity decreases rapidly with increasing frequency. That this describes the behavior of real free-electron metals is shown in Figs. 3.12 and 3.13.

The plasma frequency typically lies in the visible or ultraviolet spectral region. That corresponds to $\omega > 10^{15}$ sec^{-1}. The mean free collision time for electrons in metals is typically $\tau \approx 10^{-14}$ sec. Thus, in the region of the

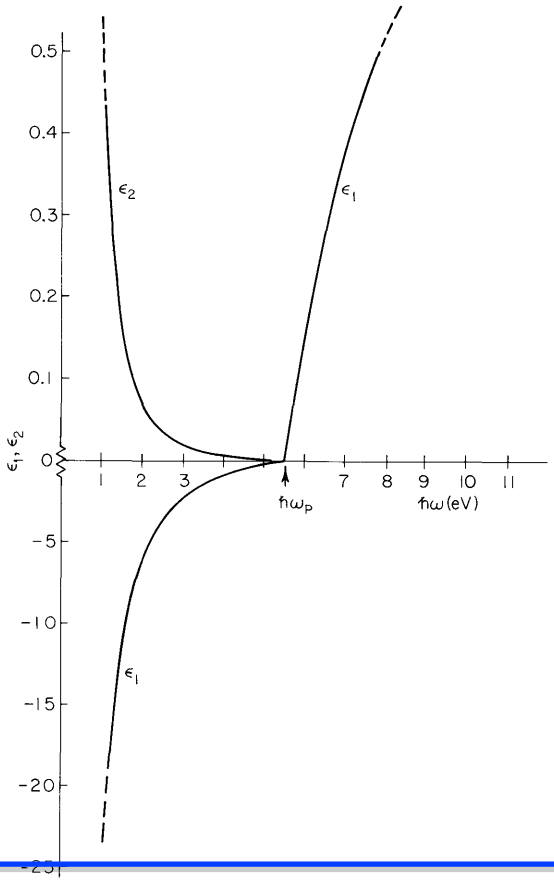

Fig. 3.8 Spectral dependence of ε_1 and ε_2 for a free-electron metal. The calculations are for the case in which $4\pi Ne^2/m = \omega_p{}^2 = 30$ eV^2 and $\hbar\Gamma = 0.02$ eV. Note the difference in scale of the ordinate along the positive and negative axes. The magnitude of ε_1 is much greater than that of ε_2 for the frequency range shown. For $\hbar\omega < \hbar\Gamma$, $|\varepsilon_2/\varepsilon_1| \to \Gamma/\omega$ and ε_2 dominates.

plasma frequency, $\omega\tau \gg 1$, and from Eq. (3.30), we get

$$\varepsilon_1 = n^2 - k^2 = 1 - (\omega_p{}^2/\omega^2) \tag{3.32}$$

From Fig. 3.9, it is clear that $n \gg k$ just above the plasma frequency and so Eq. (3.32) simplifies to

$$n^2 \approx 1 - (\omega_p{}^2/\omega^2) \tag{3.33}$$

for $\hbar\omega > \hbar\omega_p$. Just at the plasma frequency, $n \approx 0$. But what does it mean that the refractive index is zero? The index of refraction is defined in terms of the phase velocity as $v_p = c/n$. Thus, a zero value for n means an infinite

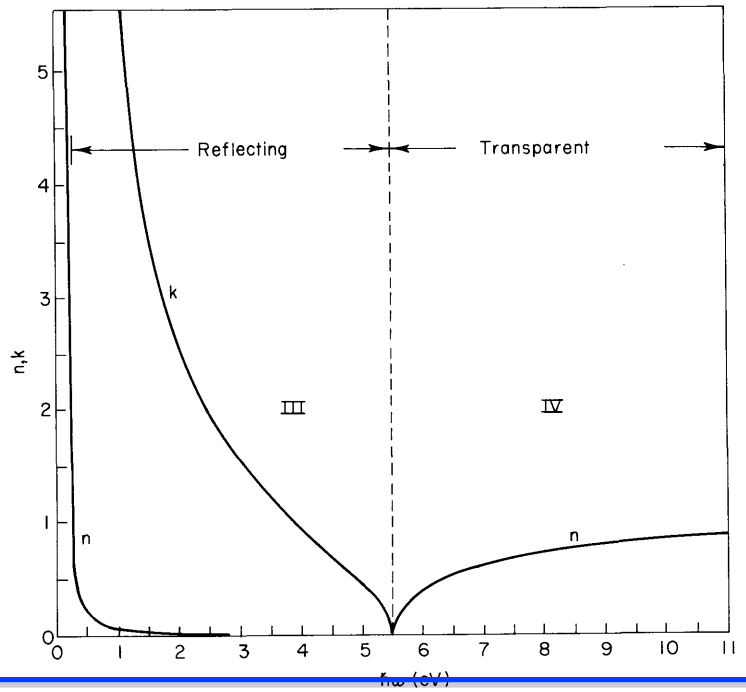

Fig. 3.9 Spectral dependence of n and k for a free-electron metal. The curves are calculated from the values of ε_1 given in Fig. 3.8. Regions III and IV correspond to the same regions as shown in Fig. 3.4. Region II, the region of strong absorption, is the range $0 \leqq \hbar\omega \leqq 0.02$ eV in this case. It is, in general, the range $0 \leqq \hbar\omega \leqq \hbar\Gamma$. Region I does not exist for metals.

phase velocity and an infinite wavelength. That the wavelength becomes infinite means the electrons are all oscillating in phase; however, there is no polarization charge density as with a true plasma oscillation. The distinction is made clear in the next section as well as in Chapter 9.

3.3 A Qualitative Look at Real Metals

We will now use the Lorentz and Drude models in a discussion of the optical behavior of some real metals. Real metals exhibit aspects of both models. To see the role of both models in describing real metals, consider the schematic band diagram for a metal as shown in Fig. 3.14.

Two typical transitions are illustrated in Fig. 3.14. The first of these, called an intraband transition, corresponds to the optical excitation of an electron from below the Fermi energy to another state above the Fermi energy but within the same band. These transitions are described by the

Drude model. There is no threshold energy for such transitions; however, they can occur only in metals. Insulators do not have partially filled bands that would allow excitation of an electron from a filled state below the Fermi energy to an empty state within the same band. That is, of course, what makes an insulator nonconducting.

The second transition illustrated in Fig. 3.14 is a direct interband transition. It is the optical excitation of an electron to another band. It is called a direct or vertical transition because it involves only the excitation of an electron by a photon. Since the momentum of a photon is very small compared with the range of values of crystal momentum in the Brillouin zone, conservation of total crystal momentum of the electron plus photon means that the value of wave vector **k** for the electron is essentially unchanged in the reduced zone scheme. There are nonvertical or indirect transitions between bands, and we shall consider them later; but for present purposes, a discussion of direct transitions is sufficient to illustrate the characteristic optical properties of real metals.

Direct interband transitions have a threshold energy. For the band

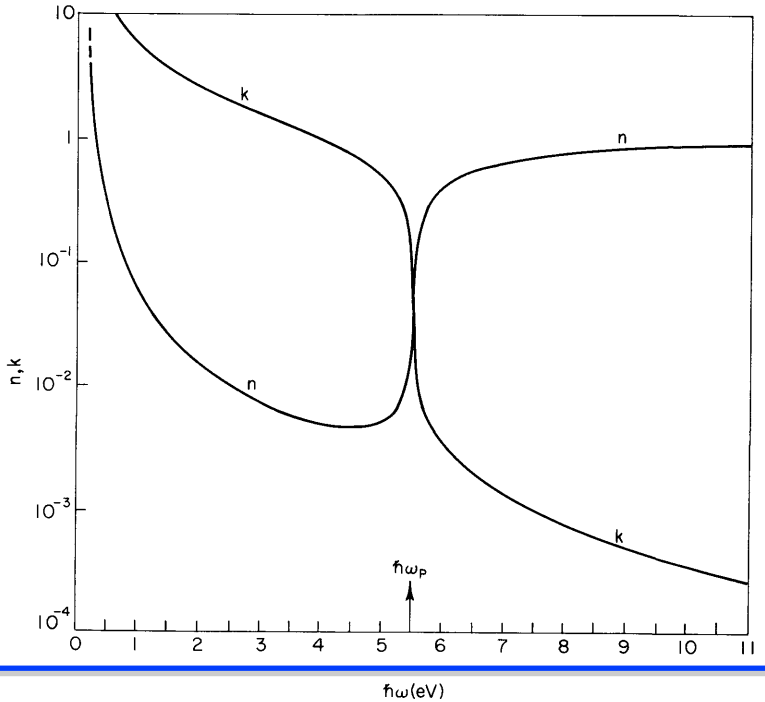

Fig. 3.10 A semilogarithmic plot of the n and k values for a free-electron metal as taken from Fig. 3.9.

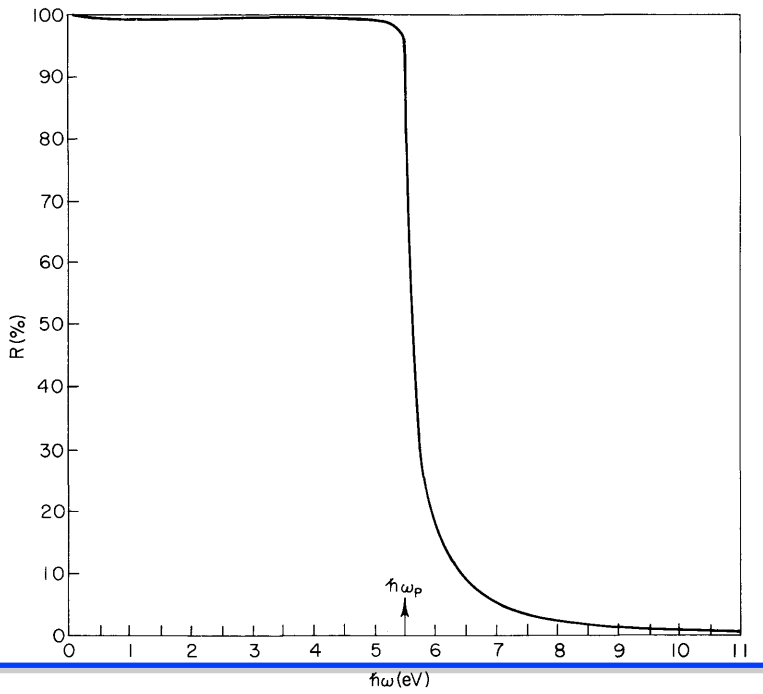

Fig. 3.11 Spectral dependence of reflectivity for a free-electron metal. The curve is calculated from the n and k values given in Fig. 3.9.

diagram shown in Fig. 3.14, the threshold energy is the energy $\hbar\omega_0$ for the transition from the Fermi energy at $\mathbf{k}_0$ to the same state $\mathbf{k}_0$ in the next higher band. This threshold energy is analogous to that for the excitation of an electron across the band gap in an insulator.

Now, how do we use these models to understand real metals, and where do we begin? The beginning is an experimental determination of the reflectance over a wide frequency range. From the reflectance, the dielectric function can be obtained using, e.g., a Kramers–Kronig analysis as discussed in Chapter 6. The dielectric function can then sometimes be split into bound (Lorentz) and free (Drude) contributions and interpreted in terms of the fundamental electronic band structure of the solid. We shall see how this can be done in some cases by following through the steps used by Ehrenreich and Philipp in their classic paper on the optical properties of silver and copper.

The reflectance of silver is shown in Fig. 3.15. A band diagram for the noble metals is shown schematically in Fig. 3.16. The d bands lie several volts below the Fermi energy. Thus, only interband transitions of conduction electrons are possible at low energies, and an onset of interband

Example 1.1

The reflectivity of silicon at 633 nm is 35% and the absorption coefficient is $3.8 \times 10^5\ \mathrm{m}^{-1}$. Calculate the transmission and optical density of a sample with a thickness of 10 μm.

Solution

The transmission is given by eqn 1.6 with $R = 0.35$ and $\alpha l = (3.8 \times 10^5) \times (10 \times 10^{-6}) = 3.8$. This gives:

$$T = (1 - 0.35)^2 \cdot \exp(-3.8) = 0.0095\,.$$

The optical density is given by eqn 1.8:

$$\text{O.D.} = 0.434 \times 3.8 = 1.65\,.$$

1.3 The complex refractive index and dielectric constant

In the previous section we mentioned that the absorption and refraction of a medium can be described by a single quantity called the **complex refractive index**. This is usually given the symbol $\tilde{n}$ and is defined through the equation:

$$\tilde{n} = n + i\kappa\,. \tag{1.11}$$

The real part of $\tilde{n}$, namely n, is the same as the normal refractive index defined in eqn. 1.2. The imaginary part of $\tilde{n}$, namely κ, is called the **extinction coefficient**. As we will see below, κ is directly related to the absorption coefficient α of the medium.

The relationship between α and κ can be derived by considering the propagation of plane electromagnetic waves through a medium with a complex refractive index. If the wave is propagating in the z direction, the spatial and time dependence of the electric field is given by (see eqn A.32 in Appendix A):

$$\mathcal{E}(z,t) = \mathcal{E}_0\, \mathrm{e}^{i(kz-\omega t)}\,, \tag{1.12}$$

where k is the wave vector of the light and ω is the angular frequency. $|\mathcal{E}_0|$ is the amplitude at $z = 0$. In a non-absorbing medium of refractive index n, the wavelength of the light is reduced by a factor n compared to the free space wavelength λ. k and ω are therefore related to each other through:

$$k = \frac{2\pi}{(\lambda/n)} = \frac{n\omega}{c}\,. \tag{1.13}$$

This can be generalized to the case of an absorbing medium by allowing the refractive index to be complex:

$$k = \tilde{n}\frac{\omega}{c} = (n + i\kappa)\frac{\omega}{c}\,. \tag{1.14}$$

On substituting eqn 1.14 into eqn 1.12, we obtain:

$$\begin{aligned}\mathcal{E}(z,t) &= \mathcal{E}_0\, \mathrm{e}^{i(\omega\tilde{n}z/c-\omega t)} \\ &= \mathcal{E}_0\, \mathrm{e}^{-\kappa\omega z/c}\, \mathrm{e}^{i(\omega n z/c-\omega t)}\,. \end{aligned} \tag{1.15}$$

This shows that a non-zero extinction coefficient leads to an exponential decay of the wave in the medium. At the same time, the real part of $\tilde{n}$ still determines the phase velocity of the wave front, as in the standard definition of the refractive index given in eqn 1.2.

The optical intensity of a light wave is proportional to the square of the electric field, namely $I \propto \mathcal{E}\mathcal{E}^*$ (c.f. eqn A.40). We can therefore deduce from eqn 1.15 that the intensity falls off exponentially in the medium with a decay constant equal to $2 \times (\kappa\omega/c)$. On comparing this to Beer's law given in eqn 1.4 we conclude that:

$$\alpha = \frac{2\kappa\omega}{c} = \frac{4\pi\kappa}{\lambda}\,, \tag{1.16}$$

where λ is the free space wavelength of the light. This shows us that κ is directly proportional to the absorption coefficient.

We can relate the refractive index of a medium to its relative dielectric constant ϵ_r by using the standard result derived from Maxwell's equations (cf. eqn A.31 in Appendix A):

$$n = \sqrt{\epsilon_\mathrm{r}}\,. \tag{1.17}$$

This shows us that if n is complex, then ϵ_r must also be complex. We therefore define the complex relative dielectric constant $\tilde{\epsilon}_\mathrm{r}$ according to:

$$\tilde{\epsilon}_\mathrm{r} = \epsilon_1 + i\epsilon_2\,. \tag{1.18}$$

By analogy with eqn 1.17, we see that $\tilde{n}$ and $\tilde{\epsilon}_\mathrm{r}$ are related to each other through:

$$\tilde{n}^2 = \tilde{\epsilon}_\mathrm{r} \tag{1.19}$$

We can now work out explicit relationships between the real and imaginary parts of $\tilde{n}$ and $\tilde{\epsilon}_\mathrm{r}$ by combining eqns 1.11, 1.18 and 1.19. These are:

$$\epsilon_1 = n^2 - \kappa^2 \tag{1.20}$$

$$\epsilon_2 = 2n\kappa\,, \tag{1.21}$$

and

$$n = \frac{1}{\sqrt{2}}\left(\epsilon_1 + (\epsilon_1^2 + \epsilon_2^2)^{\frac{1}{2}}\right)^{\frac{1}{2}} \tag{1.22}$$

$$\kappa = \frac{1}{\sqrt{2}}\left(-\epsilon_1 + (\epsilon_1^2 + \epsilon_2^2)^{\frac{1}{2}}\right)^{\frac{1}{2}}\,. \tag{1.23}$$

This analysis shows us that $\tilde{n}$ and $\tilde{\epsilon}_\mathrm{r}$ are not independent variables: if we know ϵ_1 and ϵ_2 we can calculate n and κ, and *vice versa*. Note that if the medium is only weakly absorbing, then we can assume that κ is very small, so that eqns 1.22 and 1.23 simplify to:

$$n = \sqrt{\epsilon_1} \tag{1.24}$$

$$\kappa = \frac{\epsilon_2}{2n}\,. \tag{1.25}$$

These equations show us that the refractive index is basically determined by the real part of the dielectric constant, while the absorption is mainly determined by the imaginary part. This generalization is obviously not valid if the medium has a very large absorption coefficient.

The microscopic models that we will be developing throughout the book usually enable us to calculate $\tilde{\epsilon}_r$ rather than $\tilde{n}$. The measurable optical properties can then be obtained by converting ϵ_1 and ϵ_2 to n and κ through eqns 1.22 and 1.23. The refractive index is given directly by n, while the absorption coefficient can be worked out from κ using eqn 1.16. The reflectivity depends on both n and κ and is given by

$$R = \left|\frac{\tilde{n}-1}{\tilde{n}+1}\right|^2 = \frac{(n-1)^2+\kappa^2}{(n+1)^2+\kappa^2}. \tag{1.26}$$

This formula is derived in eqn A.50. It gives the coefficient of reflection between the medium and the air (or vacuum) at normal incidence.

In a transparent material such as glass in the visible region of the spectrum, the absorption coefficient is very small. Equations 1.16 and 1.21 then tell us that κ and ϵ_2 are negligible, and hence that both $\tilde{n}$ and $\tilde{\epsilon}_r$ may be taken as real numbers. This is why tables of the properties of transparent optical materials generally list only the real parts of the refractive index and dielectric constant. On the other hand, if there is significant absorption, then we will need to know both the real and imaginary parts of $\tilde{n}$ and $\tilde{\epsilon}_r$.

In the remainder of this book we will take it as explicitly assumed that both the refractive index and the dielectric constant are complex quantities. We will therefore drop the tilde notation on n and ϵ_r from now on, except where it is explicitly needed to avoid ambiguity. It will usually be obvious from the context whether we are dealing with real or complex quantities.

Example 1.2

The complex refractive index of germanium at 400 nm is given by $\tilde{n} = 4.141 + i\,2.215$. Calculate for germanium at 400 nm: (a) the phase velocity of light, (b) the absorption coefficient, and (c) the reflectivity.

Solution

(a) The velocity of light is given by eqn 1.2, where n is the real part of $\tilde{n}$. Hence we obtain:

$$v = \frac{c}{n} = \frac{2.998\times10^8}{4.141}\,\mathrm{m\,s^{-1}} = 7.24\times10^7\,\mathrm{m\,s^{-1}}.$$

(b) The absorption coefficient is given by eqn 1.16. By inserting $\kappa = 2.215$ and $\lambda = 400\,\mathrm{nm}$, we obtain:

$$\alpha = \frac{4\pi\times2.215}{400\times10^{-9}}\,\mathrm{m^{-1}} = 6.96\times10^7\,\mathrm{m^{-1}}.$$

(c) The reflectivity is given by eqn 1.26. Inserting $n = 4.141$ and $\kappa = 2.215$ into this, we obtain:

$$R = \frac{(4.141-1)^2+2.215^2}{(4.141+1)^2+2.215^2} = 47.1\,\%.$$

Table 1.4 Composition, refractive index and ultraviolet transmission of common glasses. The letters after the names give the abbreviations used to identify the glass type. The composition figures are the percentage by mass. The refractive index is measured at 546.1 nm, and the transmission is for a 1 cm plate at 310 nm. After [1], [4].

Name	SiO_2	B_2O_3	Al_2O_3	Na_2O	K_2O	CaO	BaO	PbO	P_2O_5	n	T
Fused silica	100									1.460	0.91
Crown (K)	74			9	11	6				1.513	0.4
Borosilicate crown (BK)	70	10		8	8	1	3			1.519	0.35
Phosphate crown (PK)		3	10		12	5			70	1.527	0.46
Light flint (LF)	53			5	8			34		1.585	0.008
Flint (F)	47			2	7			44		1.607	–
Dense flint (SF)	33				5			62		1.746	–

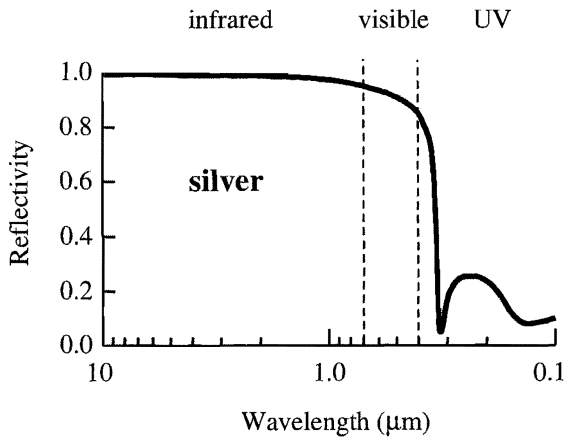

Fig. 1.5 Reflectivity of silver from the infrared to the ultraviolet. After [4].

1.4.3 Metals

The characteristic optical feature of metals is that they are shiny. This is why metals like silver and aluminium have been used for making mirrors for centuries. The shiny appearance is a consequence of their very high reflection coefficients. We will see in Chapter 7 that the high reflectivity is caused by the interaction of the light with the free electrons that are present in the metal.

Figure 1.5 shows the reflectivity of silver from the infrared spectral region to the ultraviolet. We see that the reflectivity is very close to 100 % in the infrared, and stays above 80 % throughout the whole visible spectral region. The reflectivity then drops sharply in the ultraviolet. This general behaviour is observed in all metals. There is strong reflection for all frequencies below a characteristic cut-off frequency called the plasma frequency. The plasma frequency corresponds to a wavelength in the ultraviolet spectral region, and so metals reflect infrared and visible wavelengths, but transmit ultraviolet wavelengths. This effect is called the ultraviolet transmission of metals.

Some metals have characteristic colours. Copper, for example, has a pinkish colour, while gold is yellowish. These colours are caused by interband electronic transitions that occur in addition to the free carrier effects that cause the reflection. This point will be explained in Section 7.3.2 of Chapter 7.

a greater electron affinity than hydrogen, and so the valence electrons in the O–H bond sit closer to the oxygen atoms. The two hydrogen atoms therefore possess a small positive charge which is balanced by a negative charge of twice the magnitude on the oxygen atom.

In a crystalline solid formed from the condensation of polar molecules, the atoms are arranged in an alternating sequence of positive and negative ions. The ions can vibrate about their equilibrium positions, and this produces oscillating dipole waves. These oscillations are associated with lattice vibrations, and they occur at frequencies in the infrared spectral region. We will consider the optical properties related to the lattice vibrations in detail in Chapter 10. We will see there that the light–matter interaction is associated with the excitation of phonons, which are quantized lattice waves. At this stage, we simply note that the lattice vibrations of a polar crystal give rise to strong optical effects in the infrared spectral region. These effects occur in addition to those due to the bound electrons of the atoms that comprise the crystal. In practice we can treat these two types of dipoles separately because the resonances are sharp and they occur at very different frequencies. Therefore the resonant effects of the bound electrons are negligible at the frequencies of the lattice vibrations, and *vice versa*. This point will be considered in more detail in Section 2.2.2.

2.1.3 Free electron oscillators

The electronic and vibrational dipoles considered above are both examples of bound oscillators. Metals and doped semiconductors, by contrast, contain significant numbers of free electrons. As the name implies, these are electrons that are not bound to any atoms, and therefore do not experience any restoring forces when they are displaced. This implies that the spring constant in eqn 2.2 is zero, and hence that the natural resonant frequency $\omega_0 = 0$.

The free electron model of metals is attributed to Paul Drude, and so the application of the dipole oscillator model to free electron systems is generally called the Drude–Lorentz model. The dipole oscillator model is perfectly valid, except that we must set $\omega_0 = 0$ throughout. The optical properties of free electron systems will be discussed in Chapter 7.

2.2 The dipole oscillator model

In the previous section we introduced the general assumptions of the dipole oscillator model. We now want to use the model to calculate the frequency dependence of the refractive index and absorption coefficient. This will provide a simple explanation for the dispersion of the refractive index in optical materials, and will also illustrate a very general point that the phenomena of absorption and refraction are related to each other.

2.2.1 The Lorentz oscillator

We consider the interaction between a light wave and an atom with a single resonant frequency ω_0 due to the bound electrons, as given by eqn 2.2. We

We know from experimental observations that atoms must have many natural resonant frequencies to account for the multiplicity of lines in the absorption and emission spectra. However, the salient features of the physical behaviour are well illustrated by a singly resonant system, and the inclusion of multiple resonances complicates the discussion without adding much to the physical understanding at this stage. We therefore postpone the discussion of the effects of multiple resonances to subsection 2.2.2 below.

model the displacement of the atomic dipoles as damped harmonic oscillators. The inclusion of damping is a consequence of the fact that the oscillating dipoles can lose their energy by collisional processes. In solids, this would typically occur through an interaction with a phonon which has been thermally excited in the crystal. As we will see, the damping term has the effect of reducing the peak absorption coefficient and broadening the absorption line.

The electric field of the light wave induces forced oscillations of the atomic dipole through the driving forces exerted on the electrons. We make the assumption that $m_N \gg m_0$ here so that we can ignore the motion of the nucleus. The displacement x of the electron is governed by an equation of motion of the form:

$$m_0 \frac{d^2x}{dt^2} + m_0\gamma \frac{dx}{dt} + m_0\omega_0^2 x = -e\mathcal{E}\,, \tag{2.5}$$

where γ is the damping rate, e is the magnitude of the electric charge of the electron, and $\mathcal{E}$ is the electric field of the light wave. The terms on the left hand side represent the acceleration, the damping and the restoring force respectively. The damping is modelled by a frictional force which is proportional to the velocity and impedes the motion. The term on the right hand side represents the driving force due to the AC electric field of the light wave.

We consider the interaction of the atom with a monochromatic light wave of angular frequency ω. The time dependence of the electric field is given by

$$\mathcal{E}(t) = \mathcal{E}_0 \cos(\omega t + \Phi) = \mathcal{E}_0\, \Re\mathrm{e}\left(\exp\left(-i\omega t - \Phi\right)\right), \tag{2.6}$$

where $\mathcal{E}_0$ is the amplitude and Φ is the phase of the light. In order to keep consistency with the sign convention introduced later, we have chosen to take the negative frequency part of the complex exponential.

Note that the phase factors Φ and Φ' in eqns 2.6 and 2.7 are not necessarily the same. In fact, the phase of the electrons will tend to lag behind the phase of the light. This is a well known property of forced oscillations: the vibrations occur at the same frequency as the driving force but lag behind due to the damping term. This phase lag is the origin of the slowing down of the light in the optical medium, as discussed above in Section 2.1.

The AC electric field will drive oscillations at its own frequency ω. We therefore substitute eqn 2.6 into eqn 2.5 and look for solutions of the form:

$$x(t) = X_0\, \Re\mathrm{e}\left(\exp\left(-i\omega t - \Phi'\right)\right), \tag{2.7}$$

where X_0 and Φ' are the amplitude and phase of the oscillations. We can incorporate the phase factors of eqns 2.6 and 2.7 into the amplitudes by allowing both $\mathcal{E}_0$ and X_0 to be complex numbers. We then substitute $\mathcal{E}(t) = \mathcal{E}_0 \mathrm{e}^{-i\omega t}$ into eqn 2.5, and look for solutions of the form $x(t) = X_0 \mathrm{e}^{-i\omega t}$. This gives:

$$-m_0\omega^2 X_0 \mathrm{e}^{-i\omega t} - i m_0 \gamma \omega X_0 \mathrm{e}^{-i\omega t} + m_0\omega_0^2 X_0 \mathrm{e}^{-i\omega t} = -e\mathcal{E}_0 \mathrm{e}^{-i\omega t}\,, \tag{2.8}$$

which implies that:

$$X_0 = \frac{-e\mathcal{E}_0/m_0}{\omega_0^2 - \omega^2 - i\gamma\omega}\,. \tag{2.9}$$

The displacement of the electrons from their equilibrium position produces a time varying dipole moment $p(t)$, as shown in Fig. 2.2. The magnitude of the dipole is given by eqn 2.4. This gives a resonant contribution to the macroscopic polarization (dipole moment per unit volume) of the medium. If

N is the number of atoms per unit volume, the resonant polarization is given by:

$$\begin{aligned} P_{\text{resonant}} &= Np \\ &= -Nex \\ &= \frac{Ne^2}{m_0} \frac{1}{(\omega_0^2 - \omega^2 - i\gamma\omega)} \mathcal{E} \,. \end{aligned} \tag{2.10}$$

A quick inspection of eqn 2.10 shows that the magnitude of P_{resonant} is small unless the frequency is close to ω_0. This is another general property of forced oscillations: the response is small unless the frequency is close to resonance with the natural frequency of the oscillator.

Equation 2.10 can be used to obtain the complex relative dielectric constant ϵ_r. The electric displacement $\mathbf{D}$ of the medium is related to the electric field $\boldsymbol{\mathcal{E}}$ and polarization $\mathbf{P}$ through:

$$\mathbf{D} = \epsilon_0 \boldsymbol{\mathcal{E}} + \mathbf{P}, \tag{2.11}$$

where the bold font indicates vector quantities (see eqn A.2 in Appendix A). We are interested in the optical response at frequencies close to ω_0, and so we split the polarization into a non-resonant background term and the resonant term arising from the driven response of the oscillator. We therefore write:

$$\begin{aligned} \mathbf{D} &= \epsilon_0 \boldsymbol{\mathcal{E}} + \mathbf{P}_{\text{background}} + \mathbf{P}_{\text{resonant}} \\ &= \epsilon_0 \boldsymbol{\mathcal{E}} + \epsilon_0 \chi \boldsymbol{\mathcal{E}} + \mathbf{P}_{\text{resonant}}. \end{aligned} \tag{2.12}$$

The electric susceptibility χ in eqn 2.12 accounts for all other contributions to the polarizability of the atoms. We will discuss the physical meaning of the 'non-resonant polarization' in subsection 2.2.2 below.

To simplify the mathematics, we will assume that the material is isotropic, in which case the relative dielectric constant is defined through the relationship:

$$\mathbf{D} = \epsilon_0 \epsilon_r \boldsymbol{\mathcal{E}} \,. \tag{2.13}$$

We then combine eqns 2.10–2.13 to obtain:

$$\epsilon_r(\omega) = 1 + \chi + \frac{Ne^2}{\epsilon_0 m_0} \frac{1}{(\omega_0^2 - \omega^2 - i\gamma\omega)}. \tag{2.14}$$

The treatment of non-isotropic materials only introduces unnecessary complications at this stage, and will be covered briefly in Section 2.4.

This can be spilt into its real and imaginary parts according to eqn 1.18 to give:

$$\epsilon_1(\omega) = 1 + \chi + \frac{Ne^2}{\epsilon_0 m_0} \frac{\omega_0^2 - \omega^2}{(\omega_0^2 - \omega^2)^2 + (\gamma\omega)^2} \tag{2.15}$$

$$\epsilon_2(\omega) = \frac{Ne^2}{\epsilon_0 m_0} \frac{\gamma\omega}{(\omega_0^2 - \omega^2)^2 + (\gamma\omega)^2}. \tag{2.16}$$

These formulae can be simplified further if we are working at frequencies close to resonance, where $\omega \approx \omega_0 \gg \gamma$. This allows us to approximate $(\omega_0^2 - \omega^2)$ by $2\omega_0 \Delta\omega$, where $\Delta\omega = (\omega - \omega_0)$ is the detuning from ω_0. We then notice that the low and high frequency limits of $\epsilon_r(\omega)$ are given by

$$\epsilon_r(0) \equiv \epsilon_{st} = 1 + \chi + \frac{Ne^2}{\epsilon_0 m_0 \omega_0^2}, \tag{2.17}$$

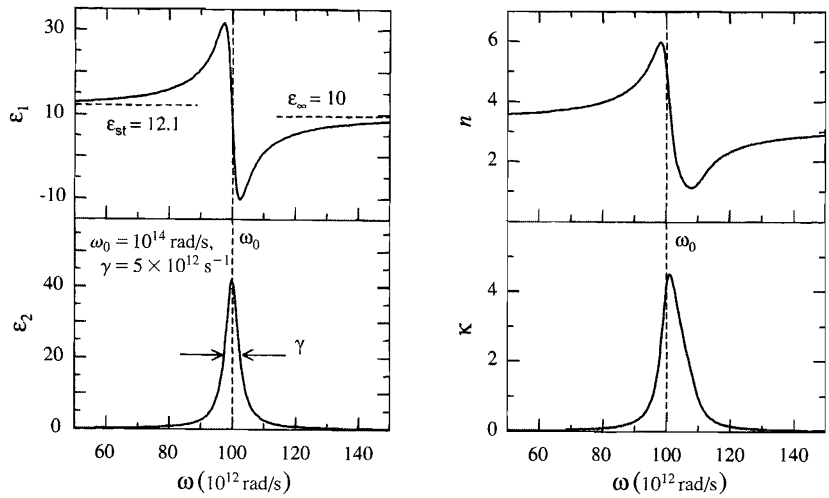

Fig. 2.4 Frequency dependence of the real and imaginary parts of the complex dielectric constant of a dipole oscillator at frequencies close to resonance. The graphs are calculated for an oscillator with $\omega_0 = 10^{14}$ rad/s, $\gamma = 5 \times 10^{12}$ s^{-1}, $\epsilon_{st} = 12.1$ and $\epsilon_\infty = 10$. Also shown is the real and imaginary part of the refractive index calculated from the dielectric constant.

and

$$\epsilon_r(\infty) \equiv \epsilon_\infty = 1 + \chi \tag{2.18}$$

respectively. The subscript on ϵ_{st} stands for 'static', since it represents the dielectric response to static electric fields. With this notation we find that:

$$(\epsilon_{st} - \epsilon_\infty) = \frac{Ne^2}{\epsilon_0 m_0 \omega_0^2}. \tag{2.19}$$

We finally rewrite eqns 2.15 and 2.16 in the following form valid at frequencies close to resonance:

$$\epsilon_1(\Delta\omega) = \epsilon_\infty - (\epsilon_{st} - \epsilon_\infty)\frac{2\omega_0 \Delta\omega}{4(\Delta\omega)^2 + \gamma^2}, \tag{2.20}$$

$$\epsilon_2(\Delta\omega) = (\epsilon_{st} - \epsilon_\infty)\frac{\gamma\omega_0}{4(\Delta\omega)^2 + \gamma^2}. \tag{2.21}$$

These equations describe a sharp atomic absorption line centred at ω_0 with full width at half maximum equal to ν.

Figure 2.4 shows the frequency dependence of ϵ_1 and ϵ_2 predicted by eqns 2.20–2.21 for an oscillator with $\omega_0 = 10^{14}$ rad/s, $\gamma = 5 \times 10^{12}$ s^{-1}, $\epsilon_{st} = 12.1$ and $\epsilon_\infty = 10$. These numbers are fairly typical of the infrared absorption lines in an ionic crystal. We see that ϵ_2 is a strongly peaked function of ω with a maximum value at ω_0 and a full width at half maximum equal to γ. The frequency dependence of ϵ_1 is more complicated. As we approach ω_0 from below, ϵ_1 gradually rises from the low frequency value of ϵ_{st}, and reaches a peak at $\omega_0 - \gamma/2$. (See Example 2.1.) It then falls sharply, passing through a minimum at $\omega_0 + \gamma/2$ before rising again to the high frequency limit of ϵ_∞. Note that the frequency scale over which these effects occur is determined by γ for both ϵ_1 and ϵ_2. This shows that the damping of the oscillator causes line broadening. The frequency dependence determined of ϵ_1 and ϵ_2 shown in Fig. 2.4 is called Lorentzian after the originator of the dipole model.

In an experiment we actually measure the refractive index n and the absorption coefficient α. The measurement of α then determines the extinction

coefficient κ through eqn 1.16. Figure 2.4 shows the values of n and κ calculated from ϵ_1 and ϵ_2 using eqns 1.22 and 1.23. We see that n approximately follows the frequency dependence of $\sqrt{\epsilon_1(\omega)}$, while κ more or less follows $\epsilon_2(\omega)$. The correspondence $n \leftrightarrow \sqrt{\epsilon_1}$ and $\kappa \leftrightarrow \epsilon_2$ would be exact if κ were much smaller than n (cf. eqns 1.24 and 1.25). This is what generally happens in gases in which the low density of atoms makes the total absorption small. In the example shown in Fig. 2.4 the correspondence is only approximate because the absorption is very strong near ω_0, so that we cannot always assume $n \gg \kappa$. Nevertheless, the basic behaviour shows that the absorption peaks at a frequency very close to ω_0 and has a width of about γ, while the refractive index shows positive and negative excursions below and above ω_0. This is the typical behaviour expected of an atomic absorption line.

One interesting aspect of the Lorentz oscillator is that it affects the refractive index over a much larger frequency range than the absorption. This point is clearly shown in the graphs given in Fig. 2.4. The absorption is a strongly peaked function of ω and falls off as $(\Delta\omega)^{-2}$ as we tune away from resonance. Thus there is no significant absorption if we tune sufficiently far from resonance. On the other hand, the frequency dependence of the refractive index varies as $|\Delta\omega|^{-1}$ for large $|\Delta\omega|$. This follows from eqn 2.20 with the approximation $n = \sqrt{\epsilon_1}$, which is valid for large $|\Delta\omega|$ when ϵ_2 is very small.

Example 2.1

The full width at half maximum of the strongest hyperfine component of the sodium D_2 line at 589.0 nm is 100 MHz. A beam of light passes through a gas of sodium with an atom density of $1 \times 10^{17}\,\mathrm{m}^{-3}$. Calculate: (i) The peak absorption coefficient due to this absorption line. (ii) The frequency at which the resonant contribution to the refractive index is at a maximum. (iii) The peak value of the resonant contribution to the refractive index.

Solution

(i) We are dealing with a low density gas of atoms, and so the approximations given in eqns 1.24 and 1.25 will be valid. This means that the absorption will directly follow the frequency dependence of $\epsilon_2(\omega)$, and the peak absorption will occur precisely at the line centre. The peak extinction coefficient can be worked out from eqns 2.16 and 1.25. This gives:

$$\kappa(\omega_0) = \frac{\epsilon_2(\omega_0)}{2n} = \frac{Ne^2}{2n\epsilon_0 m_0}\frac{1}{\gamma\omega_0}.$$

We do not know what n is, but because we are dealing with a gas, it will only be very slightly different from unity. This point is confirmed in part (iii) of the question. We therefore take $n = 1$ here, and insert $N = 1 \times 10^{17}\,\mathrm{m}^{-3}$, $\gamma = 2\pi \times 10^8\,\mathrm{s}^{-1}$ and $\omega_0 = 2\pi c/\lambda = 3.20 \times 10^{15}$ rad/s to find that $\kappa(\omega_0) = 7.90 \times 10^{-5}$. This confirms that $n \gg \kappa$, and hence that it is valid to use eqn 1.25. We then work out the absorption coefficient from Eq. 1.16, which gives:

$$\alpha_{\max} \equiv \alpha(\omega_0) = \frac{4\pi\kappa(\omega_0)}{\lambda} = 1.7 \times 10^3\,\mathrm{m}^{-1}.$$

The absorption coefficient measured in an experiment would actually be smaller than the value calculated here by about a factor of 3. This discrepancy is caused by the fact that we are assuming that the oscillator strength of the transition is unity. This point is discussed further in section 2.2.2 below.

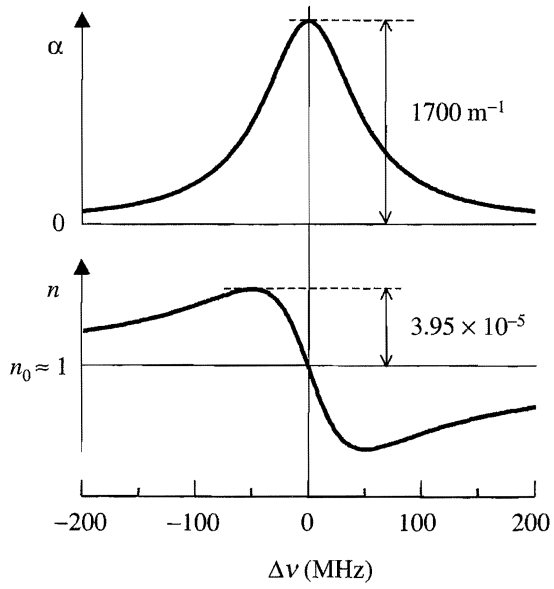

Fig. 2.5 Absorption coefficient and refractive index of sodium gas in the vicinity of the strongest hyperfine component of the D_2 line, on the assumption that the oscillator strength of the transition is unity, and that the atom density is 1×10^{17} m^{-3}. See Example 2.1 for the details. n_0 represents the off-resonant refractive index, which is approximately equal to unity.

(ii) We know from Fig. 2.4 that there will be a peak in the refractive index just below ω_0. Equation 1.24 tells us that $n(\omega) = \sqrt{\epsilon_1(\omega)}$, and hence that the local maximum of n will occur at the same frequency as the maximum in ϵ_1. Since the peak occurs near ω_0, it will be valid to use eqn 2.20. The local maximum occurs when:

$$\frac{d\epsilon_1(\omega)}{d\omega} \equiv \frac{d\epsilon_1(\Delta\omega)}{d\Delta\omega} \propto \frac{4(\Delta\omega)^2 - \gamma^2}{[4(\Delta\omega)^2 + \gamma^2]^2} = 0\,.$$

This gives $\Delta\omega = \pm\gamma/2$. We see from Fig. 2.4 that $\Delta\omega = -\gamma/2$ corresponds to the local maximum, while $\Delta\omega = +\gamma/2$ corresponds to the local minimum. Therefore the peak in the refractive index occurs 50 MHz below the line centre.

(iii) From part (ii) we know that the local maximum in the refractive index occurs when $\Delta\omega = -\gamma/2$. We see from eqns 1.24 and 2.20 that the refractive index at this frequency is given by:

$$n_{\max} = \sqrt{\epsilon_1} = \left(\epsilon_\infty + \frac{Ne^2}{2\epsilon_0 m_0 \omega_0 \gamma}\right)^{\frac{1}{2}} = n_0 \left(1 + \frac{7.90 \times 10^{-5}}{n_0^2}\right)^{\frac{1}{2}},$$

where $n_0 = \sqrt{\epsilon_\infty}$ is the off-resonant refractive index. We are dealing with a low density gas, and so it is justified to take $n_0 \approx 1$ here. This implies that the peak value of the resonant contribution to the refractive index is 3.95×10^{-5}.

The full frequency dependence of the absorption and refractive index near this absorption line is plotted in Fig. 2.5.

2.2.2 Multiple resonances

In general, an optical medium will have many characteristic resonant frequencies. We already discussed in Section 2.1 how we expect to observe separate

It can be shown from quantum mechanics that we must have $\sum_j f_j = 1$ for each electron. Since the classical model predicts $f_j = 1$ for each oscillator, we then interpret this by saying that a particular electron is involved in several transitions at the same time, and the absorption strength is being divided between these transitions.

2.2.3 Comparison with experimental data

The schematic behaviour shown in Fig. 2.6 can be compared to experimental data on a typical solid state material. Figure 2.7 shows the frequency dependence of the refractive index and extinction coefficient of fused silica (SiO_2) glass from the infrared to the X-ray spectral region. The general characteristics indicated by Fig. 2.6 are clearly observed, with strong absorption in the infrared and ultraviolet, and a broad region of low absorption in between. The data confirms that $n \gg \kappa$ except near the peaks of the absorption. This means that the approximation whereby we associate the frequency dependence of n with that of ϵ_1, and that of κ with ϵ_2 (eqns 1.24 and 1.25), is valid at most frequencies.

The general behaviour shown in Fig. 2.7 is typical of optical materials which are transparent in the visible spectral region. We already noted in Sections 1.4.1 and 1.4.2 that the transmission range of colourless materials is determined by

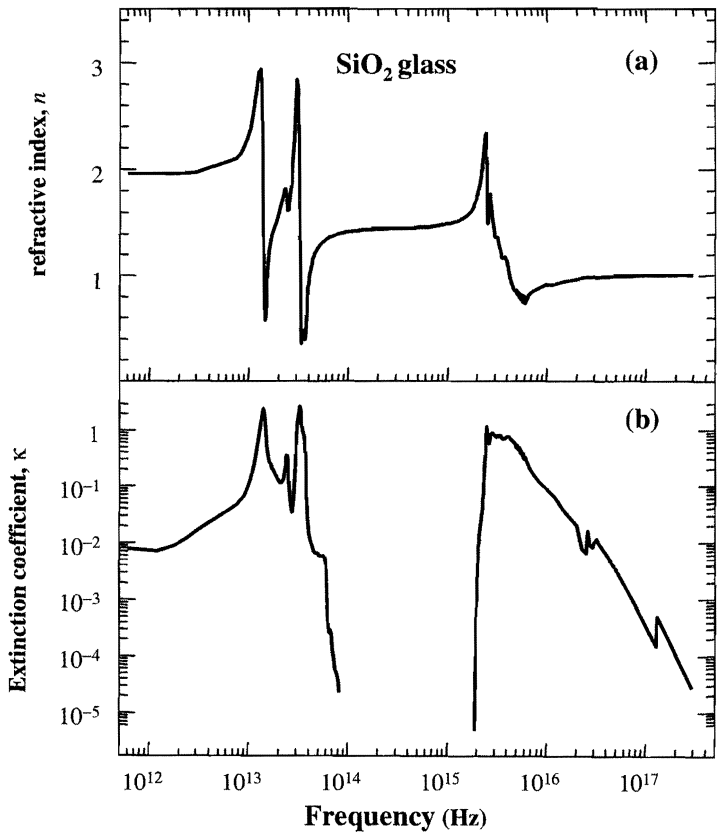

Fig. 2.7 (a) Refractive index and (b) extinction coefficient of fused silica (SiO_2) glass from the infrared to the x-ray spectral region. After [1].

the electronic absorption in the ultraviolet and the vibrational absorption in the infrared. This is demonstrated by the transmission data for sapphire shown in Fig. 1.4(a).

Silica is a glass, and hence does not have a regular crystal lattice. The infrared absorption is therefore caused by excitation of vibrational quanta in the SiO_2 molecules themselves. Two distinct peaks are observed at 1.4×10^{13} Hz (21 μm) and 3.3×10^{13} Hz (9.1 μm) respectively. These correspond to different vibrational modes of the molecule. The detailed modelling of these absorption bands by the oscillator model will be discussed in Chapter 10.

The ultraviolet absorption in silica is caused by interband electronic transitions. SiO_2 has a fundamental band gap of about 10 eV, and interband transitions are possible whenever the photon energy exceeds this value. Hence we observe an absorption threshold in the ultraviolet at 2×10^{15} Hz (150 nm). The interband absorption peaks at around 3×10^{15} Hz with an extremely high absorption coefficient of $\sim 10^8\,\mathrm{m}^{-1}$, and then gradually falls off to higher frequency. Subsidiary peaks are observed at $\sim 3 \times 10^{16}$ Hz and 1.3×10^{17} Hz. These are caused by transitions of the inner core electrons of the silicon and oxygen atoms. The fact that the electronic absorption consists of a continuous band rather than a discrete line makes it hard to model accurately as a Lorentz oscillator. We will discuss the quantum theory of the interband absorption in Chapter 3.

The refractive index of glass has resonances in the infrared and the ultraviolet which correspond to the interband and vibrational absorption. In the far infrared region below the vibrational resonance, the refractive index is ~ 2, while in the hard ultraviolet and X-ray region it approaches unity. In the transparency region between the vibrational and interband absorption, the refractive index has a value of ~ 1.5. Closer inspection of Fig. 2.7 shows that the refractive index actually increases with frequency in this transparency region, rising from a value of 1.40 at 8×10^{13} Hz (3.5 μm) to 1.55 at 1.5×10^{15} Hz (200 nm). This dispersion originates from the low frequency wings of the ultraviolet absorption and the high frequency wings of the infrared absorption, and will be discussed in more detail in Section 2.3 below.

The data in Fig. 2.7 show that the refractive index falls below unity at a number of frequencies. This implies that the phase velocity of the light is greater than c, which might seem to imply a contradiction with relativity. However, this overlooks the fact that a signal must be transmitted as a wave packet rather than as a monochromatic wave. In a dispersive medium, a wave packet will propagate at the group velocity v_g given by:

$$v_g = \frac{d\omega}{dk}, \tag{2.25}$$

rather than at the phase velocity $v = \omega/k = c/n$. The relationship between v_g and v is:

$$v_g = v\left(1 - \frac{k}{n}\frac{dn}{dk}\right). \tag{2.26}$$

The derivation of this result is left as an exercise to the reader. (See Exercise 2.7.) We will see in Section 2.3 that dn/dk is positive in most materials at optical frequencies. This then implies that v_g is always less than v, and if we were to try to transmit a signal in a spectral region where $v > c$, we

It is apparent from Fig. 2.6 that dn/dk will be negative at some frequencies close to one of the resonance lines. Equation 2.26 then implies that $v_g > v$, and so we could again run into a problem with relativity. However, the medium is highly absorbing in these frequency regions, and this means that the signal travels with yet another velocity called the signal velocity. This is always less than c.

if there is just a single resonance. This is modified to

$$\chi_a = \frac{e^2}{\epsilon_0 m_0} \sum_j \frac{f_j}{\left(\omega_j^2 - \omega^2 - i\gamma_j\omega\right)}, \tag{2.33}$$

if there are multiple resonances (cf. eqn 2.24).

We can combine eqns 2.29 and 2.30 with eqns 2.11 and 2.13 by writing

$$\mathbf{P} = N\epsilon_0\chi_a\left(\boldsymbol{\mathcal{E}} + \frac{\mathbf{P}}{3\epsilon_0}\right) = (\epsilon_r - 1)\epsilon_0\boldsymbol{\mathcal{E}}\,. \tag{2.34}$$

We put all this together to find that:

$$\frac{\epsilon_r - 1}{\epsilon_r + 2} = \frac{N\chi_a}{3}\,. \tag{2.35}$$

This result is known as the Clausius–Mossotti relationship. The relationship works well in gases and liquids. It is also valid for those crystals in which the Lorentz correction given in eqn 2.29 gives an accurate account of the local field effects, namely cubic crystals.

2.2.5 The Kramers–Kronig relationships

The discussion of the dipole oscillator shows that the refractive index and the absorption coefficient are not independent parameters but are related to each other. This is a consequence of the fact that they are derived from the real and imaginary parts of a single parameter, namely the complex refractive index. If we invoke the law of causality (that an effect may not precede its cause) and apply complex number analysis, we can derive general relationships between the real and imaginary parts of the refractive index. These are known as the Kramers–Kronig relationships and may be stated as follows:

$$n(\omega) = 1 + \frac{1}{\pi}\,\mathrm{P}\int_{-\infty}^{\infty} \frac{\kappa(\omega')}{\omega' - \omega}\,d\omega' \tag{2.36}$$

$$\kappa(\omega) = -\frac{1}{\pi}\,\mathrm{P}\int_{-\infty}^{\infty} \frac{n(\omega') - 1}{\omega' - \omega}\,d\omega', \tag{2.37}$$

where P indicates that we take the principal part of the integral.

The Kramers–Kronig relationships allow us to calculate n from κ, and *vice versa*. This can be very useful in practice, because it would allow us, for example, to measure the frequency dependence of the optical absorption and then calculate the dispersion without needing to make a separate measurement of n.

2.3 Dispersion

Figure 2.9 plots the refractive index data from Fig. 2.7 in more detail. The data show that the refractive index increases with frequency in the near infrared and visible spectral regions. We have seen in Section 2.2.3 that this dispersion originates mainly from the interband absorption in the ultraviolet. At visible

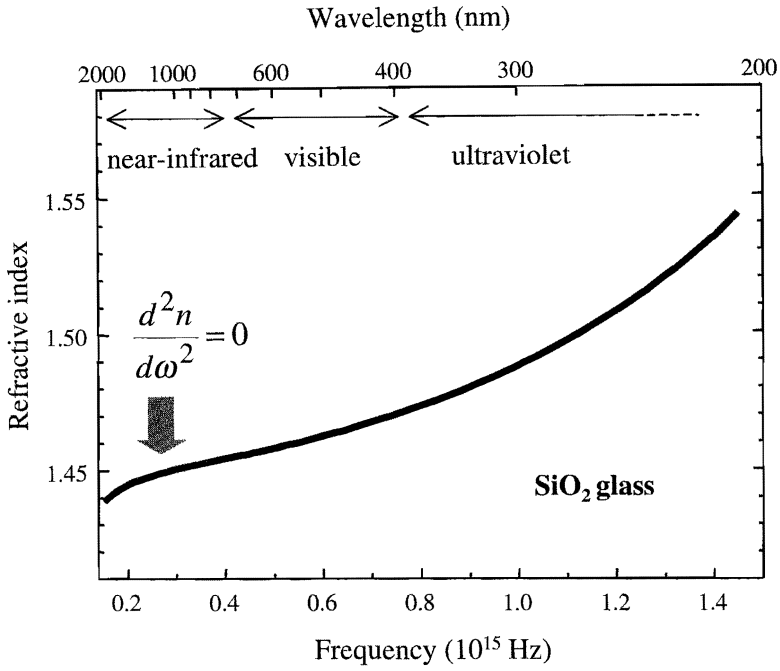

Fig. 2.9 Refractive index of SiO_2 glass in the near infrared, visible and ultraviolet spectral regions. After [1].

frequencies the absorption from these transitions is negligible and the glass is transparent. However, the ultraviolet absorption still affects the refractive index through the extreme wings of the Lorentzian line. In the near infrared, the dispersion is also affected by the high frequency wings of the vibrational absorption at lower frequency.

A material in which the refractive index increases with frequency is said to have **normal** dispersion, while one in which the contrary occurs is said to have **anomalous** dispersion. A number of empirical formulae to describe the normal dispersion of glasses have been developed over the years. (See Exercise 2.12.)

The use of the words 'normal' and 'anomalous' is somewhat misleading here. The dipole oscillator model shows us that all materials have anomalous dispersion at some frequencies. The phraseology was adopted before measurements of the refractive index had been made over a wide frequency range and the origin of dispersion had been properly understood.

The dispersion of the refractive index of glasses such as silica can be used to separate different wavelengths of light with a prism, as shown in Fig. 2.10. The blue light is refracted more because of the higher index of refraction, and is therefore deviated through a larger angle by the prism. (See Exercise 2.13.) This effect is used in prism spectrometers.

One of the effects of dispersion is that light of different frequencies takes a different amount of time to propagate through a material. (See Exercise 1.11, for example.) A pulse of light of duration t_p must necessarily contain a spread of frequencies given approximately by

$$\Delta\nu \approx \frac{1}{t_p} \tag{2.38}$$

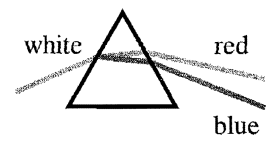

Fig. 2.10 Separation of white light into different colours by dispersion in a glass prism.

in order to satisfy the 'uncertainty principle' $\Delta\nu\Delta t \sim 1$. Dispersion will therefore cause the pulse to broaden in time as it propagates through the medium. This can become a serious problem when attempting to transmit very short pulses through a long length of an optical material, for example in a high speed optical fibre telecommunications system.

We mentioned in Section 2.2.3 that a pulse of light travels with the group velocity v_g. The important parameter for pulse spreading due to dispersion is therefore the group velocity dispersion (GVD) (see Exercise 2.14):

$$\text{GVD} = \frac{d^2\omega}{dk^2} \propto \frac{d^2n}{d\omega^2} \propto \frac{d^2n}{d\lambda^2}. \tag{2.39}$$

The Lorentz model indicates that the GVD is positive below an absorption line and negative above it. Applying this to the data in Fig. 2.9, we see negative GVD in the infrared due to the vibrational absorption and positive GVD in the visible due to the interband absorption in the ultraviolet. These two effects cancel at a wavelength in the near infrared which is identified in Fig. 2.9. This region of zero GVD occurs around 1.3 μm in silica optical fibres. Short pulses can be transmitted down the fibre with negligible temporal broadening at this wavelength, and so it is one of the preferred wavelengths for optical fibre communication systems.

2.4 Optical anisotropy: birefringence

The atoms in a solid are locked into a crystalline lattice with well defined axes. In general, we cannot assume that the optical properties along the different crystalline axes are equivalent. For example, the separation of the atoms might not be the same in all directions. This would lead to different vibrational frequencies, and hence a change in the refractive index between the relevant directions. This optical anisotropy contrasts with gases and liquids which are isotropic because the atoms have no preferred directions in the absence of external perturbations such as applied magnetic or electric fields.

Optical anisotropy gives rise to the phenomenon of birefringence. We can describe the properties of a birefringent crystal by generalizing the relationship between the polarization and the applied electric field. If the electric field is applied along an arbitrary direction relative to the crystalline axes, we must write a tensor equation to relate $\mathbf{P}$ to $\boldsymbol{\mathcal{E}}$:

$$\mathbf{P} = \epsilon_0 \boldsymbol{\chi} \boldsymbol{\mathcal{E}} \tag{2.40}$$

Equation 2.40 should be contrasted with the usual *scalar* relationship between $\mathbf{P}$ and $\boldsymbol{\mathcal{E}}$ namely (cf. eqn A.1):

$$\mathbf{P} = \epsilon_0 \chi \boldsymbol{\mathcal{E}},$$

which only applies to isotropic materials.

where $\boldsymbol{\chi}$ represents the susceptibility tensor. Written explicitly in terms of the components, we have:

$$\begin{pmatrix} P_x \\ P_y \\ P_z \end{pmatrix} = \epsilon_0 \begin{pmatrix} \chi_{11} & \chi_{12} & \chi_{13} \\ \chi_{21} & \chi_{22} & \chi_{23} \\ \chi_{31} & \chi_{32} & \chi_{33} \end{pmatrix} \begin{pmatrix} \mathcal{E}_x \\ \mathcal{E}_y \\ \mathcal{E}_z \end{pmatrix}. \tag{2.41}$$

We can simplify this by choosing the cartesian coordinates x, y, and z to correspond to the principal crystalline axes. In this case, the off-diagonal components are zero, and the susceptibility tensor takes the form:

$$\boldsymbol{\chi} = \begin{pmatrix} \chi_{11} & 0 & 0 \\ 0 & \chi_{22} & 0 \\ 0 & 0 & \chi_{33} \end{pmatrix}. \tag{2.42}$$

The relationships between the components are determined by the crystal symmetry.